HARQ Throughput Performance of DS-CDMA Using Frequency-domain ICI Cancellation

Kazuaki TAKEDA[+] and Fumiyuki ADACHI[++]
Dept. of Electrical and Communication Engineering, Graduate School of Engineering, Tohoku University
6-6-05 Aza-Aoba, Aramaki, Aoba-ku, Sendai, 980-8579 Japan
E-mail: [+]takeda@mobile.ecei.tohoku.ac.jp, [++]adachi@ecei.tohoku.ac.jp

***Abstract*—The bit error rate (BER) performance of DS-CDMA in a frequency-selective fading channel can be significantly improved by the use of frequency-domain equalization (FDE). However, the presence of a residual inter-chip interference (ICI) after FDE distorts the orthogonality among the spreading codes and the BER performance of the multicode DS-CDMA degrades as the number of multiplex order increases. The use of frequency-domain ICI cancellation can significantly improve the BER performance with FDE. In this paper, we consider hybrid automatic repeat request (HARQ) with multicode DS-CDMA using frequency-domain ICI cancellation. It is shown by computer simulation that frequency-domain ICI cancellation can significantly improve the HARQ throughput performance and reduces the required E_s/N_0 by 4~6 dB for a throughput range of 1~1.7 bit/s/Hz when QPSK modulation and SF=256 are used.**

Keywords-DS-CDMA, frequency-domain equalization, ICI cancellation, HARQ

I. Introduction

Direct-sequence code division multiple access (DS-CDMA) can exploit the channel frequency-selectivity by the use of coherent rake combining [1]. In the third generation mobile communication systems, DS-CDMA with rake combining is used for the data transmissions of up to a few Mbps. Recently, there have been great demands for data services higher than several hundreds of Mbps. However, the propagation channel for such high-speed data transmissions becomes a severe frequency-selective channel, and hence the bit error rate (BER) performance of DS-CDMA with rake combining severely degrades due to strong inter-path interference (IPI). A new equalization technique, replacing rake combining, may be required to overcome the severe frequency-selective fading channel.

Recently, it has been shown that frequency-domain equalization (FDE) based on minimum mean square error (MMSE) criterion can significantly improve the bit error rate (BER) performance of DS-CDMA in comparison to rake combining [2-4]. However, the presence of a residual inter-chip interference (ICI) after FDE distorts the orthogonality among the spreading codes and the BER performance of the multicode DS-CDMA degrades as the number of multiplex order increases. Many works on the interference cancellation combined with FDE are found in [5]-[7]. In [5], iterated-decision equalizer is presented to reduce the effect of inter-symbol interference for single-carrier transmission. In [6], frequency-domain iterative block decision feedback equalization (DFE) is presented for SC transmission. Frequency-domain interference cancellation for DS-CDMA uplink has been proposed in [7]. We have also shown that the introduction of ICI cancellation to the multicode DS-CDMA downlink is effective to improve the BER performance [8].

Recently, much attention has been paid to the high speed packet access for IP-based wireless communications [9]. Hybrid ARQ (HARQ) with rate compatible punctured turbo (RCPT) code is considered as a promising packet transmission technique [10]. It was also shown in [10] that the use of MMSE-FDE can improve the HARQ throughput performance compared to the conventional rake combining. An additional use of ICI cancellation can further improve the HARQ throughput performance. In this paper, we evaluate by computer simulation the HARQ throughput performance with multicode DS-CDMA using frequency-domain ICI cancellation.

II. Transmission System Model

A. Overall transmission system model

The DS-CDMA transmission system model is illustrated in Fig.1. At the transmitter, an information bit sequence is turbo encoded with a coding rate of R. The resultant parity sequences are punctured according to the HARQ schemes and stored in a buffer together with information bit sequence for possible retransmission. After channel interleaving and serial-to-parallel conversion, the uth code's data sequence, u=0~(U–1), is transformed into a data modulated symbol sequence $\{d_u(n)\}$ and then spread by multiplying it by an orthogonal spreading code $c_u(t)$. The resultant U chip sequences are code-multiplexed and further multiplied by a common scramble sequence $\{c_{scr}(t)\}$. After chip-interleaving using an $SF\times N_c$-chip block interleaver, the multicode DS-CDMA signal is divided into a sequence of blocks of N_c chips each and then, the last N_g chips of each block is copied as a cyclic prefix and inserted into the guard interval (GI) at the beginning of each block [2].

The GI-inserted orthogonal multicode DS-CDMA signal is transmitted over a frequency-selective fading channel and is received at a receiver. After the removal of the GI, the received chip sequence is decomposed by N_c-point FFT into N_c subcarrier components (the terminology "subcarrier" is used for explanation purpose only although subcarrier modulation is not used). After MMSE-FDE is carried out, ICI cancellation is performed in the frequency-domain. Inverse FFT (IFFT) is applied to obtain the time-domain received chip sequence for despreading and log likelihood ratio (LLR) computation. After a series of MMSE-FDE, ICI cancellation, despreading, and LLR computation is repeated a sufficient number of times, turbo decoding is performed and error detection is done in the CRC decoder. If no error is detected, the CRC decoder outputs the received data. Otherwise, retransmission is requested.

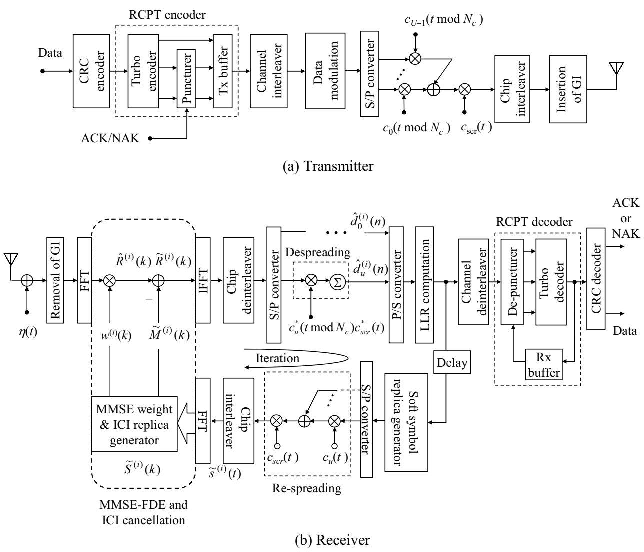

Figure 1. Transmitter/receiver structure.

B. Transmit/receive signal

Throughout this paper, chip-spaced time representation of the transmitted signals is used. Without loss of generality, a transmission of U data symbol sequences $\{d_u(n); n=0\sim N_c/SF-1\}$ is considered, where N_c and SF are chosen so that the value of N_c/SF becomes an integer. The spread signal $\{\hat{s}(t);\ t=-N_g\sim N_c-1\}$ after the GI insertion can be expressed, using the equivalent lowpass representation, as

$$\hat{s}(t)=\sqrt{2E_c/T_c}\,s(t \bmod N_c)\ \ , (1)$$

where E_c and T_c denote the chip energy and the chip duration, respectively. $s(t)$ is given by

$$s(t)=\left[\sum_{u=0}^{U-1} d_u\left(\lfloor t/SF\rfloor\right)c_u(t \bmod SF)\right]c_{scr}(t) \quad (2)$$

with $|c_u(t)|=|c_{scr}(t)|=1$ for $t=0\sim(N_c-1)$, where $\lfloor x\rfloor$ represents the largest integer smaller than or equal to x.

The propagation channel is assumed to be a frequency-selective block fading channel having chip-spaced L discrete paths, each subjected to independent fading. The assumption of block fading means that the path gains remain constant over at least one block duration. The channel impulse response $h(t)$ can be expressed as [11]

$$h(t)=\sum_{l=0}^{L-1} h_l\delta(t-\tau_l)\ \ , \ (3)$$

where h_l and τ_l are the complex-valued path gain and time delay of the lth path (l=0~L−1), respectively, with $\sum_{l=0}^{L-1} E[|h_l|^2]=1$ (E[.] denotes the ensemble average operation). We assume that the maximum time delay is shorter than the GI length (i.e., $\tau_{L-1}<N_g$). The received signal $\{r(t);\ t=-N_g\sim N_c-1\}$ can be expressed as

$$r(t)=\sum_{l=0}^{L-1} h_l\hat{s}(t-\tau_l)+\eta(t)\quad , (4)$$

where $\eta(t)$ is a zero-mean complex Gaussian process with a variance of $2N_0/T_c$ with N_0 being the single-sided power spectrum density of the additive white Gaussian noise (AWGN) process.

C. MMSE-FDE and ICI cancellation

A joint MMSE-FDE and ICI cancellation is repeated in an iterative fashion. Below, the ith iteration is described.

After the removal of the GI from the received signal $r(t)$, N_c-point FFT is applied to decompose $\{r(t);t=0\sim N_c-1\}$ into N_c subcarrier components $\{R(k);\ k=0\sim N_c-1\}$. The kth subcarrier component $R(k)$ can be written as

$$\begin{aligned}R(k)&=\sum_{t=0}^{N_c-1} r(t)\exp\left(-j2\pi k\frac{t}{N_c}\right)\\&=H(k)S(k)+\Pi(k)\end{aligned}\ , (5)$$

where $S(k)$, $H(k)$ and $\Pi(k)$ are the kth subcarrier component of the transmitted signal $\{s(t);\ t=0\sim N_c-1\}$ of N_c chips, the channel gain and the noise due to the AWGN, respectively, and are given by

$$\begin{cases}S(k)=\sum_{t=0}^{N_c-1} s(t)\exp\left(-j2\pi k\dfrac{t}{N_c}\right)\\ H(k)=\sqrt{\dfrac{2E_c}{T_c}}\sum_{l=0}^{L-1} h_l\exp\left(-j2\pi k\dfrac{\tau_l}{N_c}\right)\\ \Pi(k)=\sum_{t=0}^{N_c-1}\eta(t)\exp\left(-j2\pi k\dfrac{t}{N_c}\right)\end{cases}\ . \ (6)$$

MMSE-FDE is carried out as

$$\begin{aligned}\hat{R}^{(i)}(k) &= w^{(i)}(k)R(k) \\ &= S(k)\hat{H}^{(i)}(k) + \hat{\Pi}^{(i)}(k)\end{aligned} \quad (7)$$

with

$$\begin{cases}\hat{H}^{(i)}(k) = w^{(i)}(k)H(k) \\ \hat{\Pi}^{(i)}(k) = w^{(i)}(k)\Pi(k)\end{cases}, (8)$$

where $w^{(i)}(k)$ is the equalization weight at the ith iteration and $\hat{H}^{(i)}(k)$ and $\hat{\Pi}^{(i)}(k)$ are the equivalent channel gain and the noise, after performing MMSE-FDE at the ith iteration, respectively. The MMSE weight is given by [8]

$$w^{(i)}(k) = \frac{H^*(k)}{|H(k)|^2 \rho^{(i-1)} + 2\sigma^2}, (9)$$

where $\rho^{(i-1)}$ is an interference factor and $\rho^{(-1)} = 1$ ($\rho^{(i-1)}$ is derived in Sect. IV).

ICI cancellation is performed as

$$\tilde{R}^{(i)}(k) = \hat{R}^{(i)}(k) - \tilde{M}^{(i)}(k), (10)$$

where $\tilde{M}^{(i)}(k)$ is the residual ICI replica, and is given by [8]

$$\tilde{M}^{(i)}(k) = \begin{cases}0 & \text{for } i = 0 \\ \{\hat{H}^{(i)}(k) - A^{(i)}\}\tilde{S}^{(i-1)}(k) & \text{for } i \geq 1\end{cases}, (11)$$

where $\tilde{S}^{(i-1)}(k)$ is the kth frequency component of the transmitted chip replica generated by feeding back a decision variable of the (i–1)th iteration stage and $A^{(i)}$ is given by

$$A^{(i)} = \frac{1}{N_c}\sum_{k=0}^{N_c-1}\hat{H}^{(i)}(k). (12)$$

D. Despreading and LLR computaion

N_c-point IFFT is applied to transform the frequency-domain signal $\{\tilde{R}^{(i)}(k); k = 0 \sim N_c - 1\}$ into the time-domain signal $\{\tilde{r}^{(i)}(t); t = 0 \sim N_c - 1\}$:

$$\tilde{r}^{(i)}(t) = \frac{1}{N_c}\sum_{k=0}^{N_c-1}\tilde{R}^{(i)}(k)\exp\left(j2\pi t\frac{k}{N_c}\right). (13)$$

After despreading, the uth user's decision variable associated with $d_u(n)$ is obtained as

$$\hat{d}_u^{(i)}(n) = \frac{1}{SF}\sum_{t=nSF}^{(n+1)SF-1}\tilde{r}^{(i)}(t)c_u^*(t \bmod SF)c_{scr}^*(t). (14)$$

Using $\hat{d}_u^{(i)}(n)$, the log-likelihood ratio (LLR) for the xth bit in the nth symbol $d_u(n)$ (n=0~N_c/SF–1), where x=0~ $(\log_2\Omega) - 1$ and Ω is the modulation level, is computed as [12]

$$L_x^{(i)}(n) \approx \frac{\left|\hat{d}_u^{(i)}(n) - A^{(i)}d_{b_{n,x}=0}^{\min}\right|^2}{2\hat{\sigma}^2} - \frac{\left|\hat{d}_u^{(i)}(n) - A^{(i)}d_{b_{n,x}=1}^{\min}\right|^2}{2\hat{\sigma}^2},(15)$$

where $d_{b_{n,x}=0}^{\min}$ (or $d_{b_{n,x}=1}^{\min}$) is the most probable symbol that gives the minimum Euclidean distance from $\hat{d}_u^{(i)}(n)$ among all the candidate symbols $\{d\}$ with $b_{n,x} = 0$ (or 1). $2\hat{\sigma}^2$ is the variance of the noise plus residual ICI.

After a series of MMSE-FDE, ICI cancellation, and despreading, turbo decoding is performed using $L_x^{(i)}(n)$ and error detection is done in the CRC decoder. If no error is detected, the CRC decoder outputs the received data. Otherwise, retransmission is requested.

III. ICI Replica Generation and MMSE Weight

We consider the i(≥1)th iteration. ICI replica generation is presented. Then, the MMSE weight taking into account the residual ICI is derived.

A. ICI replica generation

The soft decision variable is used to generate the replica $\{\tilde{s}^{(i-1)}(t); t = 0 \sim N_c - 1\}$ of the transmitted chip sequence so as to avoid the error propagation due to the decision feedback of decision errors. For QPSK data modulation and 16-quadrature amplitude modulation (16QAM), the soft symbol replica $\{\tilde{d}_u^{(i-1)}(n)$;n=0~N_c/SF–1} can be obtained as [8]

$$\begin{cases}\tilde{d}_u^{(i-1)}(n) = \frac{1}{\sqrt{2}}\tanh\left(\frac{L_0^{(i-1)}(n)}{2}\right) + j\frac{1}{\sqrt{2}}\tanh\left(\frac{L_1^{(i-1)}(n)}{2}\right) \\ \qquad \text{for QPSK} \\ \tilde{d}_u^{(i-1)}(n) = \frac{1}{\sqrt{10}}\tanh\left(\frac{L_0^{(i-1)}(n)}{2}\right)\left\{2 + \tanh\left(\frac{L_1^{(i-1)}(n)}{2}\right)\right\} \\ \qquad + j\frac{1}{\sqrt{10}}\tanh\left(\frac{L_2^{(i-1)}(n)}{2}\right)\left\{2 + \tanh\left(\frac{L_3^{(i-1)}(n)}{2}\right)\right\} \\ \qquad \text{for 16QAM}\end{cases}.(16)$$

The replica $\{\tilde{s}^{(i-1)}(t); t = 0 \sim N_c - 1\}$ of the transmitted chip sequence $s(t)$ is generated as

$$\tilde{s}^{(i-1)}(t)=\left[\sum_{u=0}^{U-1}\tilde{d}_u^{(i-1)}(\lfloor t/SF\rfloor)c_u(t \bmod SF)\right]c_{scr}(t) \quad .(17)$$

Then, N_c-point FFT is applied to decompose the replica $\tilde{s}^{(i-1)}(t)$ into N_c subcarrier components $\{\tilde{S}^{(i-1)}(k);k=0\sim(N_c-1)\}$ as

$$\tilde{S}^{(i-1)}(k)=\sum_{t=0}^{N_c-1}\tilde{s}^{(i-1)}(t)\exp\left(-j2\pi k\frac{t}{N_c}\right) \quad .(18)$$

Substituting Eq. (18) into Eq. (11), we obtain the frequency-domain ICI replica $\tilde{M}^{(i)}(k)$.

B. MMSE weight and interference factor

To derive the MMSE weight taking into account the residual ICI, we define the equalization error $e(k)$ between the frequency component $\{\tilde{R}^{(i)}(k);k=0\sim N_c-1\}$ after the ICI cancellation and the transmitted frequency component $\{S(k);k=0\sim N_c-1\}$ as

$$e(k)=\tilde{R}^{(i)}(k)-A^{(i)}S(k) \quad ,(19)$$

where $A^{(i)}S(k)$ is used as a reference signal since $E[\tilde{R}^{(i)}(k)]=A^{(i)}S(k)$ (the residual ICI is assumed to be zero-mean). We want to derive the weight that minimizes the mean square error (MSE) $E[|e(k)|^2]$ for the given $H(k)$, i.e., $\partial E[|e(k)|^2]/\partial w^{(i)}(k)=0$. The following MMSE weight is obtained as

$$w^{(i)}(k)=\frac{H^*(k)}{|H(k)|^2\rho^{(i-1)}+2\sigma^2} \quad , (20)$$

where

$$\rho^{(i-1)}=\sum_{t=0}^{N_c-1}\left\{|s(t)|^2-|\tilde{s}^{(i-1)}(t)|^2\right\}. \quad (21)$$

Since $s(t)$ is unknown, we use the hard decision chip sequence replica $\bar{s}^{(i-1)}(t)$ instead of $s(t)$ in Eq. (21).

IV. HARQ

RCPT HARQ type II *S-P2* [10] is considered, as shown in Fig. 2. In type II *S-P2*, two parity bit sequences of K bits, obtained by the turbo encoder, are punctured with the period of two to generate two different parity bit sequences of K bits. The puncturing matrix for type II *S-P2* is given by

$$\begin{bmatrix}1&1\\0&0\\0&0\end{bmatrix}\begin{bmatrix}0&0\\1&0\\0&1\end{bmatrix}\begin{bmatrix}0&0\\0&1\\1&0\end{bmatrix} \quad .(22)$$

In the first transmission, the information bit sequence of K bits is only transmitted and MMSE-FDE and ICI cancellation are performed. If errors are detected, the first punctured parity bit sequence is transmitted as the 2nd transmission. Hence, the turbo decoding of R=1/2 can be carried out at the receiver. For the 3rd transmission, the second punctured parity sequence is transmitted and the turbo decoding of R=1/3 is performed.

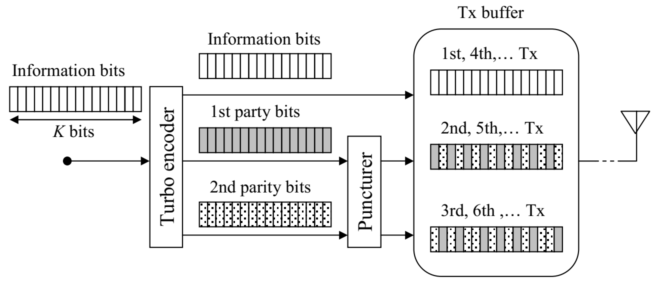

Figure 2. HARQ Type II *S-P4*.

V. COMPUTER SIMULATION

The turbo encoder with (13,15) RSC encoders and a log-MAP decoder with 8 iterations are used. The length of information bit sequence is K=1024 bits. QPSK data modulation and 16QAM, N_c=256, N_g=32, and an L=16-path frequency-selective Rayleigh fading channel having uniform power delay profile ($E[|h_l|^2]=1/L$) are assumed. Ideal sampling timing and ideal channel estimation are assumed at the receiver.

TABLE I. SIMULATION PARAMETERS

Transmitter	Modulation	QPSK, 16QAM
	Number of FFT points	N_c=256
	GI	N_g=32(chip)
	Spreading sequence	Product of Walsh sequence and PN sequence
	Spreading factor	SF=U=1, 16 and 256
Channel	Fading	Frequency-selective block Rayleigh fading
	Power delay profile	L=16-path uniform power delay profile
Receiver	Channel estimation	Ideal
Turbo coding	Encoder	(13,15)RSC encoder
	Decoder	Log-MAP decoding
	Number of iteration	8 iterations

The simulated throughput performances of DS-CDMA with and without ICI cancellation are plotted in Fig. 3 as a function of the average received symbol energy-to-AWGN noise power spectrum density ratio E_s/N_0 for SF=U=1, 16 and 256. For QPSK (see Fig. 3 (a)), frequency-domain ICI cancellation can significantly improve the throughput performance for E_s/N_0>10 dB. In such a high E_s/N_0 region, the predominant cause of the throughput degradation is the residual ICI and hence, the throughput can be improved by ICI cancellation. However, in a low E_s/N_0 region, the throughput cannot be improved since the predominant cause of the throughput degradation is the noise rather than the residual ICI. When *SF*=*U*=16 and 256, a slightly better throughput than *SF*=1 is obtained since the residual ICI is better suppressed by the despreading process. When *SF*=256, an E_s/N_0 reduction of about 4~6 dB can be achieved for a throughput range of 1~1.7 bit/s/Hz.

For 16QAM (see Fig. 3 (b)), the Euclidean distance between different data symbols is shorter and hence, decision error due to the residual ICI is more likely than for QPSK. Therefore, frequency-domain ICI cancellation is very effective to improve the throughput performance for 16QAM as well. When *SF*=256, an E_s/N_0 reduction of about 4~6 dB can be achieved for a throughput range of 2~3 bit/s/Hz.

VI. CONCLUSION

In this paper, frequency-domain ICI cancellation was introduced to HARQ using multicode DS-CDMA with MMSE-FDE and the throughput performance was evaluated by computer simulation. It was shown that ICI cancellation can improve the throughput performance in a high E_s/N_0 region since the predominant cause of the throughput degradation is the residual ICI. However, in a low E_s/N_0 region, ICI cancellation cannot improve the throughput since the predominant cause of the throughput degradation is the noise rather than the residual ICI. When *SF*=256, an E_s/N_0 reduction of about 4~6 dB can be achieved for a throughput range of 1~1.7 (2~3) bit/s/Hz for QPSK (16QAM).

REFERENCES

[1] J. G. Proakis, *Digital communications*, 3rd edition, McGraw-Hill, 1995..

[2] F. Adachi, D. Garg, S. Takaoka, and K. Takeda, “Broadband CDMA techniques,” IEEE Wireless Communications Magazine, Vol. 12, No. 2, pp.8-18, April. 2005.

[3] F. W. Vook, T. A. Thomas, and K. L. Baum, “Cyclic-prefix CDMA with antenna diversity,” Proc. IEEE VTC 2002 Spring, pp. 1002-1006, May 2002.

[4] I. Martoyo, G. M.A. Sessler, J. Luber and F. K. Jondral, “Comparing equalizers and multiuser detections for DS-CDMA downlink systems,” Proc. IEEE VTC 2004-Spring, May 2004.

[5] A. M. Chan and G. W. Wornell, “A class of block-iterative equalizers for intersymbol interference channels: fixed channel results,” IEEE Trans. Commun., vol. 49, no. 11, pp. 1966-1976, Nov. 2001.

[6] N. Benvenuto and S. Tomasin, “Block iterative DFE for single carrier modulation,” IEE Electronics Letters, vol. 38, no. 19, pp. 1144-1145, Sept. 2002.

[7] S. Tomasin and N. Benvenuto, “Frequency-domain interference cancellation and nonlinear equalization for CDMA systems,” IEEE Trans. Wireless Commun., vol. 4, no. 5. pp. 2329-2339, Sept. 2005.

[8] K. Takeda, K. Ishihara, and F. Adachi, “Downlink DS-CDMA transmission with joint MMSE equalization and ICI cancellation,” Proc. IEEE VTC 2006-spring, Melbourne, Australia, 7-10 May 2006, to be published.

[9] H. Atarashi, S. Abeta and M. Sawahashi, “Variable spreading orthogonal frequency and code division multiplexing (VSF-OFCDM) for broadband packet wireless access,” IEICE Trans. Commun., Vol. E86-B, pp. 291-299, Jan. 2003.

[10] D. Garg and F. Adachi, “Comparison of Rcpt HARQ Throughpyt Using OFDM, MC-CDMA and DS-CDMA with Frequency-domain Equalization,” Proc. 9th IEEE International Conference on Communications Systems (ICCS 2004), Singapore, 6-8 Sep, 2004.

[11] T. S. Rappaport, *Wireless communications*, Prentic Hall, 1996.

[12] A. Stefanov and T. Duman, “Turbo coded modulation for wireless communications with antenna diversity,” Proc. IEEE VTC99-Fall, pp.1565-1569, Netherlands, Sept. 1999.

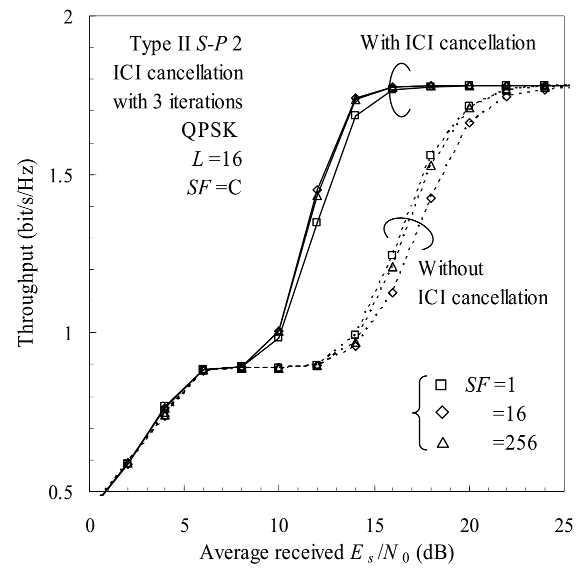

(a) QPSK

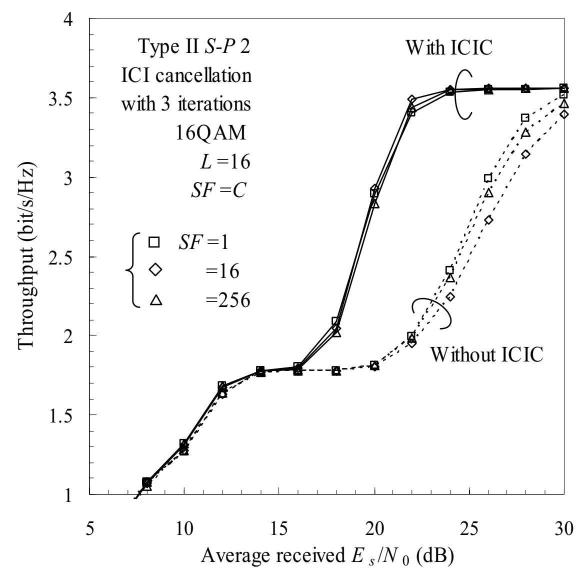

(b) 16QAM

Figure 3. HARQ throuput performance.